Long-lived localized field configurations in small lattices: Application to oscillons

M. Gleiser*

Department of Physics and Astronomy, Dartmouth College, Hanover, New Hampshire 03755

A. Sornborger†

NASA/Fermilab Astrophysics Group, Fermi National Accelerator Laboratory, Box 500, Batavia, Illinois 60510-0500

(Received 30 August 1999)

Long-lived localized field configurations such as breathers, oscillons, or more complex objects naturally arise in the context of a wide range of nonlinear models in different numbers of spatial dimensions. We present a numerical method, which we call the *adiabatic damping method*, designed to study such configurations in small lattices. Using three-dimensional oscillons in ϕ^4 models as an example, we show that the method accurately (to one part in 10^5 or better) reproduces results obtained with static or dynamically expanding lattices, dramatically cutting down in integration time. We further present results for two-dimensional oscillons, whose lifetimes would be prohibitively long to study with conventional methods.

PACS number(s): 05.10.−a, 11.27.+d, 05.45.Yv, 47.11.+j

I. INTRODUCTION

The study of long-lived, localized coherent configurations is of great interest to many areas of physics and engineering. In general, these structures arise within the context of numerical studies of effective nonlinear field models, which may describe behavior either already observed in the laboratory or conjectured to exist in phenomena yet to be observed. In contrast to the usual solitonic behavior, which is marked by localized time-independent configurations, these are time-dependent configurations, which nevertheless persist for very long times. It is reasonable to suppose that the long lifetimes are due to energy exchange promoted by nonlinear coupling between different modes which efficiently suppresses the radiation of energy away from the configuration. One may collectively call these *persistent coherent field configurations* (PCFCs) in order to distinguish them from the usual static coherent configurations that characterize solitonic behavior.

Perhaps the most well-known PCFCs are the one-dimensional breathers that appear during low-velocity kink-antikink interactions in sine-Gordon and ϕ^4 models [1]. These are bound states characterized by nonlinear oscillations about the energy minimum (or vacuum) of the model, typically one of the minima in a degenerate double-well potential. As argued by Campbell *et al.*, breathers should form when the kinks have enough time to lose energy through their interaction, adjusting to their new trapped state. It is thus expected that these bound states form for small relative velocities for the kink-antikink pair, although the dependence on the velocity is far from trivial [2]. Once the breather forms, it will remain in its oscillatory state for a remarkably long time, with minimal emission of radiation. We are not aware of a detailed study of the lifetimes of these

configurations for obvious reasons: it would take a huge amount of integration time in order to follow the evolution of these bound states until their demise. The nonlinear nature of the problem also has precluded (at least so far) analytical estimates for breather lifetimes.

In the mid-1970s, three-dimensional, breatherlike configurations were discovered in the context of ϕ^4 models by Bogolubsky and Makhankov [3]. These authors found that, for certain initial conditions, spherically symmetric bubbles settled into long-lived configurations that they called pulsons. In 1994, one of us rediscovered these configurations while studying the collapse of subcritical bubbles in the context of degenerate and nondegenerate ϕ^4 models [4]. Since the typical behavior characterizing these configurations is the high-frequency oscillation about the global minimum of the model, the name *oscillon* was chosen instead. A further detailed analysis revealed more of the remarkable behavior of these configurations, such as the dependence of lifetime on initial radius, the minimal radius for the bubbles to settle into oscillonic behavior, and the mechanism for their final demise [5]. Recent work has pointed out the possible relevance of these structures for resonant hadronic states [6].

These configurations are far from being constrained to relativistic nonlinear field theories. Remarkably similar behavior has been found in experiments involving grains (or ''sand'') placed on a plate undergoing sinusoidal vibrations [7]. These PCFCs were independently named oscillons, and their discovery has triggered a host of theoretical work attempting to model the experimental results. These include molecular dynamics simulations [8], semicontinuum theories [9], Ginzburg-Landau models [10], coupled-map models [11], order-parameter models [12], and other continuum models [13]. The difficulty here is in obtaining macroscopic laws describing the motion of granular materials, which can exhibit both solid and fluid properties. Oscillonic behavior has also been found in studies of acoustic instabilities in stars [14]. Long-lived, spatially extended oscillatory behavior appears to be bringing together research in traditionally very distant fields of physics.

*Electronic address: gleiser@dartmouth.edu

†Present address: Laboratory for Applied Mathematics, Mt. Sinai School of Medicine, One Gustav L. Levy Place, New York, NY 10029. Electronic address: ats@camelot.mssm.edu

Our goal in this paper is to present a method that is extremely useful in the study of PCFCs arising in the context of nonlinear wave models. The numerical challenge arises due to the peculiar nature of these configurations; although they are well localized, they do radiate some of their energy, which, for small lattices, will get reflected back, compromising the numerical results. Furthermore, a large amount of energy may be shed initially as the field (or fields) settles (settle) into a PCFC. The simplest approach is to set up a very large spatial lattice, large enough that the outward radiation will never hit the boundary within the integration time. Clearly, this approach (used in [4]) is extremely inefficient for very long-lived PCFCs. An improvement is to use dynamically expanding lattices, that is, lattices that grow ahead of the radiation [5]. This saves some time, but not much as the lifetime becomes fairly large. Clearly, for more detailed studies of these objects, a more efficient numerical method is badly needed, one that allows for an accurate study of very long-lived PCFCs with relatively small lattices. Although we will introduce the method within the context of d-dimensional spherically symmetric models, it can be easily implemented in more complex situations.

The paper is organized as follows. In the next section we present in detail the numerical integration routine we used, the fourth-order operator splitting method developed in Ref. [15]. This is followed by a discussion of the adiabatic damping method we propose for studying long-lived configurations in small lattices. In Sec. III we use three-dimensional oscillons to test the accuracy of the adiabatic damping method by comparing its performance with results obtained from dynamically expanding lattices. In Sec. IV we present an analytical estimate for the minimum radius for the onset of two-dimensional oscillonic behavior. This estimate is then tested numerically in Sec. V, where we also display the result for the lifetime of a few oscillons, which live at least three orders of magnitude longer than their three-dimensional counterparts. We conclude in Sec. VI with a summary of our results and directions for future work.

II. NUMERICAL TECHNIQUES

A. Fourth-order symplectic method

The Hamiltonian field equations for our theory are

$$\dot{\pi} = \partial_\rho^2 \phi + \frac{(d-1)}{\rho} \partial_\rho \phi - \partial_\phi V(\phi) \tag{1}$$

and

$$\dot{\phi} = \pi, \tag{2}$$

where d is the number of spatial dimensions, and $V(\phi)$ is the potential, taken to be a function of the field ϕ. To integrate these equations, we use a higher-order operator splitting method, which is symplectic for Hamiltonian systems. In brief, symplectic methods use the fact that Hamiltonian systems of equations can be written as

$$\dot{z} = \{z, H\}, \tag{3}$$

where the vector $z = (\pi_i, \phi_i)$ (in our case, $i = 1$, so we drop the i's), and where $\{a, b\}$ is a Poisson bracket. Now, we define the operator D_H by $D_H z \equiv \{z, H\}$. The equations become

$$\dot{z} = D_H z, \tag{4}$$

which, integrating for time Δt, has the formal solution

$$z(t + \Delta t) = e^{\Delta t D_H} z(t). \tag{5}$$

Note that, in general, systems of first-order equations can also be written in the form (4). However, the phase-space behavior of nonsymplectic systems is usually singular. In general, D_H is a sum of terms $D_H = D_1 + D_2 + \cdots + D_N$. To some order in Δt, we can approximate the exponential of a sum of operators as a product of exponentials, where each exponential has one of the operators as its argument. We use the notation

$$(\Delta t) \tag{6}$$

to represent

$$(e^{\Delta t D_1} e^{\Delta t D_2} \cdots e^{\Delta t D_N}) \tag{7}$$

and

$$(\Delta t)^T \tag{8}$$

to represent

$$(e^{\Delta t D_N} \cdots e^{\Delta t D_2} e^{\Delta t D_1}). \tag{9}$$

So, for example, the second-order method

$$(e^{\Delta t D_1} e^{\Delta t D_2} \cdots e^{\Delta t D_N})(e^{\Delta t D_N} \cdots e^{\Delta t D_2} e^{\Delta t D_1}) \tag{10}$$

is represented by

$$(\Delta t)(\Delta t)^T. \tag{11}$$

In this paper, we use an explicit fourth-order method for ''splitting'' the operator $\exp(D_H \Delta t)$. The method is [15]

$$(\Delta t)^T (\Delta t)(\Delta t)^T (-2\Delta t)(\Delta t)^T (\Delta t)^T (\Delta t)^T (\Delta t)$$
$$\times (\Delta t)^T (\Delta t)(\Delta t)(\Delta t)(\Delta t)(-2\Delta t)^T (\Delta t)(\Delta t)^T (\Delta t).$$
$$\tag{12}$$

We split the Hamiltonian $H = \pi^2 + (\nabla \phi)^2 + V(\phi)$ into two parts, $H_1 = (\nabla \phi)^2 + V(\phi)$ and $H_2 = \pi^2$. The action of the operator $\exp(\Delta t D_2)$ on z is

$$\dot{\phi} = \{\phi, H_2\} = \{\phi, H\} = \pi,$$
$$\dot{\pi} = 0, \tag{13}$$

which corresponds to integrating Eq. (14),

$$\phi^{n+1} = \phi^n + \Delta t \pi^n, \tag{14}$$

where the superscript n indicates the time step, while leaving the value of π the same. Note that this integration is exact for these equations. The action of the operator $\exp(\Delta t D_1)$ on z is

$$\dot{\phi} = 0,$$

$$\dot{\pi} = \{\pi, H_1\} = \{\pi, H\} = \left(\partial_\rho^2 \phi^n + \frac{(d-1)}{\rho} \partial_\rho \phi^n - \partial_\phi V^n \right),$$ (15)

which corresponds to integrating Eq. (16),

$$\pi^{n+1} = \pi^n + \Delta t \left(\partial_\rho^2 \phi^n + \frac{(d-1)}{\rho} \partial_\rho \phi^n - \partial_\phi V^n \right)$$ (16)

(we use fourth-order spatial differences for the derivative terms), while leaving the value of ϕ the same. Higher-order methods combine the integration of these equations in such a manner as to cancel higher-order errors in the commutators $[D_1, D_2]$.

The standard leapfrog method is a second-order symplectic method. To see this from our notation, we write

$$(\tfrac{1}{2}\Delta t)(\tfrac{1}{2}\Delta t)^T = (e^{\Delta t D_1/2} e^{\Delta t D_2/2})(e^{\Delta t D_2/2} e^{\Delta t D_1/2})$$

$$= (e^{\Delta t D_1/2} e^{\Delta t D_2} e^{\Delta t D_1/2}),$$ (17)

where $D_1 \pi = \{\pi, H\}$ and $D_2 \phi = \{\phi, H\}$. Over the course of a simulation, we have

$$z_{final} = (e^{\Delta t D_1/2} e^{\Delta t D_2} e^{\Delta t D_1} e^{\Delta t D_2} \cdots e^{\Delta t D_1} e^{\Delta t D_2} e^{\Delta t D_1/2})$$

$$\times z_{initial}.$$ (18)

Therefore, by first setting the momenta at the half time step, the leapfrog method is to alternate the integration of the ϕ's and π's, and then finally to correct the momenta by a half time step. Higher-order methods such as the fourth-order method above require both swapping and integration with negative time steps.

The expected error in ϕ and π from our method is $RN\Delta t^5$, where R is a coefficient of order $O(1)$ given by the particular method and N is the number of time steps in the simulation [15]. To test the above fourth-order method, we run a simulation with $N = 650\,000$ time steps, where $\Delta t = 0.01$ on an expanding grid. Our expected error at the end of the simulation is of order $(6.5 \times 10^{-5})R$. To measure the actual accuracy of the method, we calculate the change in energy $\delta E/E$ over the duration of the simulation and find a value $\delta E/E = 4 \times 10^{-4}$ over 6500 time units, or $650\,000$ time steps, which is compatible with the expected error.

B. Adiabatic damping method: Small lattices for long simulations

In order to decrease the size of the grid, we want to absorb the nonlinear radiation propagating away from the oscillon. For a problem involving massless radiation, we could use absorbing boundary conditions. However, for the problem at hand, the radiation is nonlinear, with a different dispersion relation for different wave modes. Therefore, we introduce a damping term at a sufficient distance away from
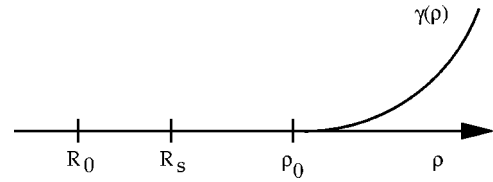

FIG. 1. A schematic diagram for the relevant spatial scales in the implementation of the ADM. R_0 is the linear scale of the PCFC, R_s is the location of the shell where the energy of the PCFC is measured, and ρ_0 is the starting point of the damping term. Units are set by the particular interactions and dimensionality of the system.

the oscillon such that the evolution of the oscillon is not disturbed, while the outgoing radiation is absorbed [the adiabatic damping method (ADM)]. This gives us a new equation of motion,

$$\ddot{\phi} + \gamma(\rho)\dot{\phi} - \nabla^2 \phi + V'(\phi) = 0.$$ (19)

The introduction of the nonzero decay term gives us a new equation for π,

$$\pi^{n+1} = \frac{1}{1 + \gamma(\rho)\Delta t/2} \left[\frac{\pi^n}{1 - \gamma(\rho)\Delta t/2} \right.$$

$$\left. + \Delta t \left(\partial_\rho^2 \phi^n + \frac{(d-1)}{\rho} \partial_\rho \phi^n - \partial_\phi V^n \right) \right].$$ (20)

Here, γ is a function of ρ. We set $\gamma = 0$ for all gridpoints less than ρ_0. For gridpoints greater than ρ_0, we set $\gamma = \eta^2(\rho - \rho_0)^2$, where η is a *small* constant. We note that the idea of adiabatic switching of a linearly increasing dissipation has been investigated for discrete breathers in Hamiltonian lattices [16]. For the successful implementation of the method, it is crucial that ρ_0 be chosen far enough away from the PCFC so as not to interfere with its dynamics. We find that, for a typical linear scale characterizing the PCFC of R_0, a safe choice is $\rho_0 \gtrsim 20 R_0$, although different situations may call for different choices of ρ_0. In Fig. 1, we present a diagram of the relevant scales for the partition of the spatial lattice.

The introduction of the damping term reduces our method from a symplectic method to an operator splitting method, since the phase space of the system no longer obeys Liouville's theorem.

The smallness of η ensures the very slow increase of the effective damping with the radial direction. (Hence the name *adiabatic damping method.*) This method can easily be generalized for higher dimensional lattices of different geometry. The ρ dependence of γ was chosen such that the first derivative was zero at ρ_0. This choice gave us better accuracy than, for instance, a constant or an exponential dependence on radius.

We should remark that the adiabatic damping equations are mixed hyperbolic-parabolic. It has been claimed that [17], since all higher-order operator splitting methods have operators with backward evolution in time, operator splitting methods of order greater than 2 are unstable for parabolic problems. Clearly, this is incorrect. We were able to integrate

our mixed hyperbolic-parabolic equations for extremely long times (over 10^9 time steps) and found no instability. It is also clear why these methods are stable. The total backward time integration in our method is $4\Delta t$, but the method integrates forward in time for $16\Delta t$. Therefore, any instability arising from exponential increase in mode amplitudes from backward-time integration will be resuppressed by the forward-time integration.

III. TESTING THE ADIABATIC DAMPING METHOD WITH THREE-DIMENSIONAL OSCILLONS

The Lagrangian for our field theory is

$$L = \pi \int (2r)^{(d-1)} dr [\tfrac{1}{2}\dot{\phi}^2 - \tfrac{1}{2}\phi'^2 - V(\phi)], \qquad (21)$$

where d is the number of spatial dimensions (for us $d=2$ or $d=3$ only), and we use the degenerate double-well potential

$$V(\phi) = \frac{\lambda}{4}(\phi^2 - \phi_{vac}^2)^2. \qquad (22)$$

As shown in [4,5], oscillons can easily be found by setting the initial field configuration with a Gaussian or a tanh profile. Here, we will use the Gaussian ansatz,

$$\phi = (\phi_c - \phi_{vac})e^{-\rho^2/R_0^2} + \phi_{vac}, \qquad (23)$$

where R_0 is the core radius and ϕ_{vac} is the asymptotic vacuum value of the field. ϕ_c sets the offset of the field from the vacuum at the core, the central displacement from equilibrium.

The evolution of the configuration can be divided into three stages. Initially, the field sheds enough energy to settle (or not, if the initial parameters R_0 and ϕ_c are outside the allowed range for oscillonic behavior) into the oscillon configuration. The lifetime of the oscillon stage is sensitive to the choices of R_0 and ϕ_c, although the energy of the configuration is not. This is, in fact, what justifies identifying these PCFCs as a single configuration. We conjecture that the lifetime of the oscillon configuration can be traced to the perturbations induced by the different choices of initial parameters, which will tend to increase the amount of radiation being emitted. However, we so far have not been able to prove this. The final stage is the oscillon's demise. As shown in Ref. [4], due to the small but steady radiation from the oscillon, at some point the maximum amplitude allowed (that is, when $\dot{\phi}_c=0$) falls approximately below the inflection point of the potential, the motion becomes linear, and $\phi_c \to \phi_{vac}$ exponentially fast.

As one would expect, one must understand something about the evolution of the oscillon to correctly set ρ_0, since damping must not interfere with the evolution of the oscillon. As a rule of thumb, the better localized the configuration, the closer ρ_0 can be to R_0. The fact that oscillons behave asymptotically as $\exp(-\rho)$ certainly helps. As remarked above, we found that $\rho_0 = 20R_0$ worked well.

To make sure that the damping region we have introduced does not interfere with the evolution of the oscillon, we checked that the oscillon lifetime is not significantly differ-
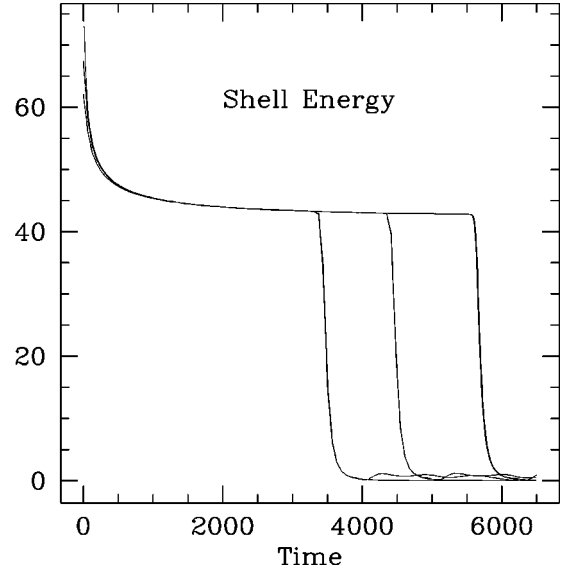

FIG. 2. Shell energy vs time: The evolution of the energy in a shell of radius $R_s = 5R_0$ about the oscillon core as a function of time. Two graphs are superimposed, the exact solution and the solution using a small 1024 point grid with damping. From left to right, we see the curves for $R_0 = 2.5$, 2.6, and 2.7. Time and space are given in units of $\lambda^{1/2}\phi_{vac}$. Energy is given in units of $\phi_{vac}/\sqrt{\lambda}$.

ent on grids with damping. We simulate oscillons on two grids. One simulation is performed on an expanding grid ($\Delta x = 0.2$), the other on a 1024 point grid with physical size 204.8 ($\Delta x = 0.2$), where the damping with constant $\eta = 0.005$ begins at $\rho = 20R_0$. In Fig. 2, we have superimposed the graph of an expanding grid simulation, which we take to be the exact result, and the approximate result, which comes from a simulation with a damping region for several choices of initial radii R_0. (All physical quantities are quoted in dimensionless units. For three-dimensional relativistic field theories, distance and time are given in units of $\lambda^{-1/2}\phi_{vac}^{-1}$.) The plots denote the time evolution of the total energy in a shell about the core (we have set our shell at $R_s = 5R_0$).

As is apparent from Fig. 2, oscillon lifetimes are essentially indistinguishable for the time spacings of the data output in these graphs. Evolution of oscillons generated from initial configurations with larger radii agrees less well with the exact oscillons due to a greater interaction between long-wavelength modes, generated as the oscillon decays at the end of its lifetime, and the reflecting boundary at the far end of the damped part of the grid. This can be cured by using a larger grid and increasing ρ_0. Notwithstanding these considerations, the agreement in lifetimes is still extremely good for 1024 gridpoints, as is shown next. The reason that long-wavelength modes introduce difficulties with this method is that they are damped less efficiently than short-wavelength modes [the damping is roughly proportional to $\exp(-k^2 t)$].

In Fig. 3, we plot the logarithm (base 10) of the absolute value of $\Delta E_s/E_s$ as a function of time, where E_s is the energy in a shell of radius $5R_0$ about the origin. We chose $R_0 = 2.7$ in this example. ΔE_s is the difference between the energies of the expanding grid simulation and the damped simulation. The shell energies agree with each other to better than one hundredth of a percent until the oscillon decays.
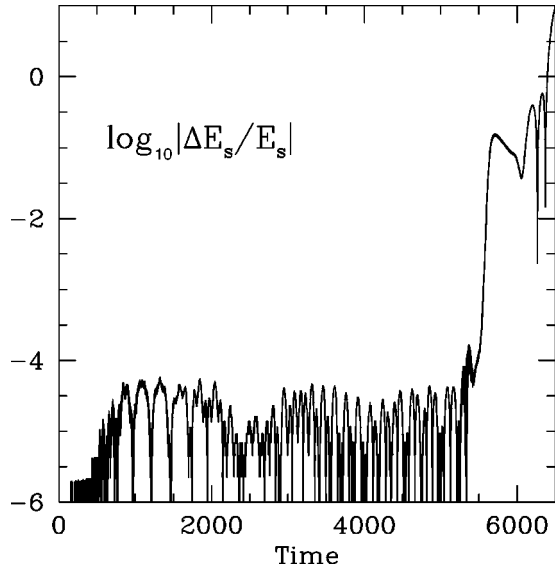
FIG. 3. $\Delta E_s/E_s$ vs time: The relative difference between the expanding grid and damped grid solutions as a function of time for $R_0=2.7$. Note that through all of the lifetime of the oscillon the solutions agree to better than one-hundredth of a percent. The logarithm is base 10, and time is in units of $\lambda^{1/2}\phi_{vac}$.

IV. ANALYTICAL ESTIMATE FOR ONSET OF TWO-DIMENSIONAL OSCILLONS

In order to estimate the approximate minimum size at which oscillonlike PCFCs appear in a two-dimensional nonlinear field theory, we begin with the ansatz

$$\phi(r,t)=A(t)e^{-r^2/R_0^2}+\phi_{vac}, \qquad (24)$$

where $A(t)\equiv\phi_c(t)-\phi_{vac}$. The Lagrangian for our field theory is given in Eq. (21) with $d=2$, and the potential is given in Eq. (22) as in the case for three-dimensional (3D) oscillons. This ansatz restricts the time dependence to the amplitude at the core of the configuration, taking the radius to be a constant parameter. Despite its simplicity, reducing a field theory to a model with one degree of freedom, it was used successfully for determining the minimum radius of 3D oscillons in Ref. [5].

Substituting the ansatz (24) into the Lagrangian and integrating over the radial dimension gives an effective Lagrangian for the single degree of freedom $A(t)$,

$$L=2\pi\left(\frac{R_0^2}{8}\dot{A}^2-\frac{1}{4}A^2-\frac{R_0^2}{32}A^4+\frac{R_0^2}{6}A^3-\frac{R_0^2}{4}A^2\right). \quad (25)$$

The equation of motion is

$$\ddot{A}+\frac{2}{R_0^2}A+2A+\frac{1}{2}A^3-2A^2=0. \qquad (26)$$

We then assume that we can separate $A(t)=A_0(t)+\delta A(t)$ and investigate harmonic perturbations about the background (assumed stable) solution $A_0(t)$. This leads to a frequency response of
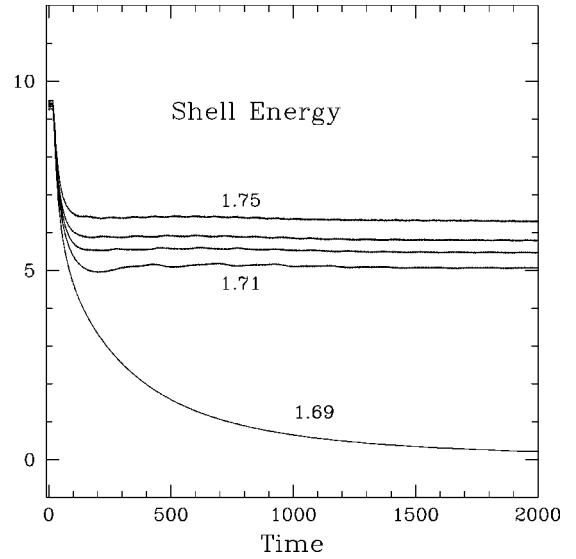

FIG. 4. Shell energy vs time: The evolution of the energy in a shell of radius $R_s=5R_0$ about the oscillon core as a function of time. Initial conditions were, from bottom to top, $R_0=1.69$, 1.71, 1.72, 1.73, and 1.75. Energy is in units of ϕ_{vac}^2, while space and time are in units of $\sqrt{\lambda}\,\phi_{vac}$.

$$\omega^2(A_0,R_0)=2+\frac{2}{R_0^2}+\frac{3}{2}A_0^2-4A_0. \qquad (27)$$

If we now minimize the frequency as a function of A_0, we find

$$\omega^2(A_0^{\min},R_0)=\frac{2}{R_0^2}-\frac{2}{3}. \qquad (28)$$

We expect an instability to develop for $\omega^2<0$, giving a bifurcation at $R_0=\sqrt{3}$: oscillons can only exist in the presence of these instabilities, which ensure the (temporary) survival of the nonlinear regime. This is reminiscent of the well-known spinodal instability in Ginzburg-Landau systems, where the growth of instabilities occurs as the system probes the concave part of the potential (or free-energy density) [18]. In short, although the perturbed solution is exponentially increasing for this linear analysis, we expect nonlinear terms to stabilize it, at least temporarily, leading to oscillon solutions. As we will see below, this prediction is quite accurate.

V. RESULTS FOR TWO-DIMENSIONAL OSCILLONS

We can now use the adiabatic damping method to study two-dimensional oscillons, which preliminary studies (with large lattices) have shown to be remarkably long lived. (Previous simulations were stopped as lifetimes went over $\tau\sim10^4$ time units.) In Fig. 4, we plot the energy in a shell of radius $R_s=5R_0$ about the origin as a function of time. Starting with Gaussian initial configurations, we searched for oscillons around $R_0=\sqrt{3}$, the expected onset value of the oscillon solution obtained above, and found the bifurcation at the slightly lower value of $R_0\simeq1.71$, as indicated in the figure.

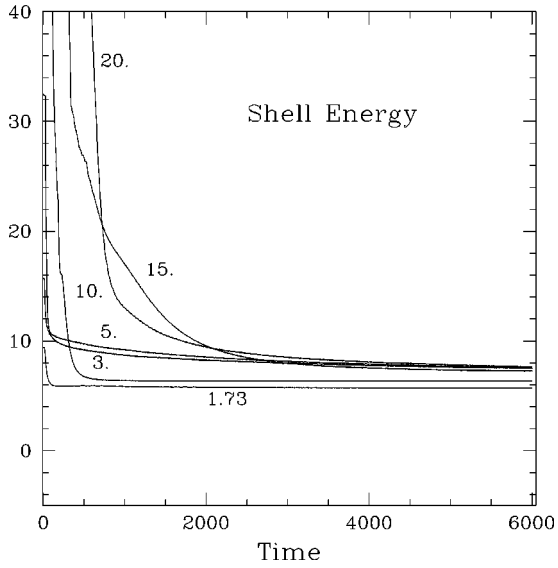Above this value for the initial radius, our results exhibit

FIG. 5. Shell energy vs time: Examples of several 2D oscillons. The radii for the initial Gaussian profiles are noted by each curve. Energy is in units of ϕ_{vac}^2, while space and time are in units of $\sqrt{\lambda}\,\phi_{vac}$.
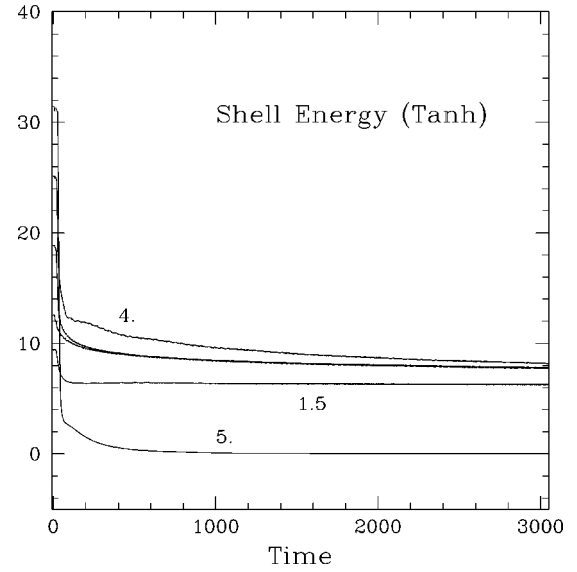

FIG. 6. Shell energy vs time: Examples of several 2D oscillons from a tanh initial configuration. The initial radii are noted by each curve, with $R_0=2$ and 3 omitted for clarity. Energy is in units of ϕ_{vac}^2, while space and time are in units of $\sqrt{\lambda}\,\phi_{vac}$.

the same behavior as for the three-dimensional oscillons, with a few different and surprising properties, which are easily identified in Fig. 5. First, we could not find a maximum radius above which the initial configurations do not become oscillons. (We searched all the way to $R_0=30$.) We recall that for 3D oscillons obtained from Gaussian initial configurations, the maximum radius was $R_0\simeq4.2$ [5]. We suspect this peculiar behavior to be a consequence of the fact that, in two dimensions, Gaussian configurations have constant surface energy densities, that is, no radial dependence. (For 2D Gaussians, the energy varies as $E=A+BR_0^2$, where A and B depend on the potential.) For initial configurations with tanh profiles, we found oscillons within the interval $1.5\lesssim R_0 \lesssim4.5$, as indicated in Fig. 6. We note that tanh configurations with small radii are fairly well approximated by Gaussian configurations, that is, have small surface energy terms.

Second, the energy plateau is not as clearly defined as in the 3D case. For example, a configuration with initial radius $R_0=10$ evolves into a lower-energy oscillon than the other cases in the figure. Also, the oscillon energy for the marginal case $R_0=1.73$ is lower than the rest. This suggests that there may exist several ''excited,'' or metastable, oscillonic states in two-dimensional models, something worth pursuing.

Third, we also could not find a finite lifetime for the oscillons. Using the adiabatic damping method, we followed the evolution of the oscillons for over 10^7 time units without observing their demise. (With our time steps this implies more than 2×10^9 time iterations.) This strongly suggests that these may be time-dependent stable solutions. We are currently pursuing this issue in more detail, using both analytical and numerical methods. We note that, in theories with conserved particle number, simple time-dependent solutions known as nontopological solitons have been found [19]. However, in the case at hand, the conserved quantity giving rise to the (possible) stability of the configuration is not immediately obvious.

VI. SUMMARY AND OUTLOOK

We have presented a method designed for the numerical investigation of long-lived field configurations such as breathers, oscillons, and other spatially extended persistent coherent field configurations. The method uses an adiabatically increasing damping term in the equation of motion, placed safely away from the PCFC so as not to interfere with its dynamics. We argue that, with this method, it is possible to follow the dynamical evolution of these objects for extremely long times, allowing us to obtain accurate results with very small lattices. Using three-dimensional oscillons as an example, we showed that the method allows for accuracies of a fraction of a percent in the measurement of physical quantities, such as the energy and lifetime, typically of the order of one part in 10^5. We then applied this approach to investigate two-dimensional oscillons. After obtaining the minimum radius that allows for their existence, we discovered that lifetimes can exceed 10^7 time units. Although not yet proven, it is possible that these time-dependent field configurations are absolutely stable.

There are quite a few obvious avenues for future work, in addition to the ones mentioned above. It would be straightforward to apply the method to more complex geometries, for example, searching for tubelike oscillons, or the study of interactions between oscillons, similar to one-dimensional kink-antikink scattering studies. As mentioned elsewhere, these configurations may be thermally nucleated during phase transitions, leading to important corrections to decay rates and completion times [20]. Given the longevity of 2D oscillons, this may be particularly relevant to systems in the two-dimensional Ising universality class. It would also be interesting to study ''excited oscillons,'' that is, non-spherically-symmetric configurations which can be expanded into a series of harmonics. Do these configurations decay into their ground state (a normal, $\ell=0$ oscillon) or are they completely unstable? It is hoped that future research will establish the connection between the various oscillons de-

scribed in the literature as obeying some simple general principles.

[1] Y. S. Kivnar and B. A. Malomed, Rev. Mod. Phys. **61**, 763 (1989); S. Flach and C. R. Willis, Phys. Rep. **295**, 181 (1998); *Solitons*, edited by S. E. Trullinger, V. E. Zakharov, and V. L. Prokovsky (North-Holland, Amsterdam, 1986).

[2] D.K. Campbell, J. F. Schonfeld, and C.A. Wingate, Physica D **9**, 1 (1983).

[3] I. L. Bogolubsky and V. G. Makhankov, Pis'ma Zh. Éksp. Teor. Fiz. **24**, 15 (1976) [JETP Lett. **24**, 12 (1976)]; **25** 120 (1977) [**25**, 107 (1977)]; V. G. Makhankov, Phys. Rep., Phys. Lett. **35C**, 1 (1978).

[4] M. Gleiser, Phys. Rev. D **49**, 2978 (1994).

[5] E. J. Copeland, M. Gleiser, and H.-R. Müller, Phys. Rev. D **52**, 1920 (1995).

[6] J. N. Hormuzdiar and S. D. H. Hsu, Phys. Rev. C **59**, 889 (1999); e-print hep-th/9906058.

[7] F. Melo, P. Umbanhowar, and H. L. Swinney, Phys. Rev. Lett. **72**, 172 (1994); **75**, 3838 (1995); P. Umbanhowar, F. Melo, and H. L. Swinney, Nature (London) **382**, 793 (1995).

[8] C. Bizon, M. D. Shattuck, J. B. Swift, W. D. McCormick, and H. L. Swinney, Phys. Rev. Lett. **80**, 57 (1998).

[9] D. H. Rothman, Phys. Rev. E **57**, 1239 (1998); E. Cerda, F. Melo, and S. Rica, Phys. Rev. Lett. **79**, 4570 (1997).

[10] L. S. Tsimring and I. S. Aranson, Phys. Rev. Lett. **79**, 213 (1997).

[11] S. C. Venkataramani and E. Ott, Phys. Rev. Lett. **80**, 3495 (1998).

[12] C. Crawford and H. Riecke, Physica D **129**, 1 (1999).

[13] J. Eggers and H. Riecke, Phys. Rev. E **59**, 4476 (1999).

[14] O. M. Umurhan, L. Tao, and E. A. Spiegel, e-print astro-ph/9806209.

[15] A. Sornborger and E. Stewart, e-print quant-ph/9903055.

[16] S. Flach, K. Kladko, and C. R. Willis, Phys. Rev. E **50**, 2293 (1994).

[17] Q. Sheng, IMA J. Numer. Anal. **9**, 199 (1989).

[18] J. D. Gunton, M. San Miguel and P. S. Sahni, in *Phase Transitions and Critical Phenomena*, edited by C. Domb and J. L. Lebowitz (Academic Press, London, 1983), Vol. 8.

[19] R. Friedberg, T. D. Lee, and A. Sirlin, Phys. Rev. D **13**, 2739 (1976); S. Coleman, Nucl. Phys. B **262**, 263 (1985).

[20] M. Gleiser and A. F. Heckler, Phys. Rev. Lett. **76**, 180 (1996).